



20 A 24 DE MAIO DE 2018 SALVADOR – BA – BRASIL

DEVELOPING FLOW IN THE INLET REGION OF BIFURCATIONS IN MICROCHANNELS WITH SYMMETRIC ANGULATION

Flavio Peres Amado¹, flavioam@petrobras.com.br; fpamado@live.estacio.com.br

Mila Rosendarl Avelino², mila.avelino@pq.cnpq.br

Jordana Colman³, jordanacolman@yahoo.com.br

Ediomedson Sales de Lucena¹, ediomedson@hotmail.com, ediomedson@hotmail.com

Narcisio Gragory dos Santos Mazzarela¹, narcisio.gregory@gmail.com

¹Universidade Estacio de Sá, Rua Eduardo Luiz Gomes, 134 - Morro do Estado, Niterói - RJ, 24020-340

²Universidade do Estado do Rio de Janeiro – UERJ, Cx. Postal 68503, Rio de Janeiro - RJ, 21945-970;

³Universidade Federal do Rio de Janeiro – UFRJ, Centro de Tecnologia - Av. Horácio Macedo, 2030, Cidade Universitária, Rio de Janeiro - RJ, 21941-450

Abstract: *The aim of this work is to evaluate the behavior of the velocity fields and predict the length of the not fully developed flow region, in the inlet of symmetric bifurcations of rectangular sectioned microchannels. An equation found in specialized literature, developed for prediction in conventional and thin curved tubes, was tested. This formulation was adapted for microtubes. Three experimental micro-devices were utilized, each fork with a larger side and a thinner side. The channel widths, flow rates and bifurcation angles were varied. Flowing were simulated via finite difference method and the lengths of the region were measured and compared to the values calculated through the proposed equation. The obtained results allowed to conclude that the equation predicts with good accuracy the length of the region of flow development, for a range of angles between 30 and 60 degrees. For the case of flow variation, it was possible to conclude that it predicted with good coincidence of results flow rates between $1.39 \times 10^{-10} \text{ m}^3/\text{s}$ and $5.56 \times 10^{-10} \text{ m}^3/\text{s}$. In dimensional terms, bifurcations with outlets widths smaller than $200 \mu\text{m}$ have shown the best agreement. The applicability of the equation for asymmetric bifurcations is recommendable to be tested in future works.*

Keywords: *Flow development, Microchannel, Bifurcation*

1. BIBLIOGRAPHIC BASIS

Flow behavior in geometries with small diameter passages is well documented and often relied upon in a practical system. The compressibility effects, slip boundary condition, and the rarefied flow concerns do not apply for a considerable quantity of single-phase liquid flows in microchannels, despite the pressure drop explicitly depends on the hydraulic resistance. In Avelino et al, 2016, it is assumed that the continuum assumption is valid for water flowing in microchannels larger than $1.0 \mu\text{m}$ in hydraulic diameter.

The region of flow development in processes that need to be laminar is of utmost importance because it translates into turbulence after any obstacle existing along the flow path. These obstacles could be valves, bends, bifurcations, meters, i.e., all constraints, commonly found in several ducted flow schemes. Specifically, in microchannels, bifurcations are very common. An example is the complex of veins and arteries that make up the circulatory system of vertebrate living organisms, in that parts where the blood circulation must not be turbulent, for the correct distribution of red blood cells in the body, as evidenced by Cameron and Skofronick, 1978.

Once it is a premise that the continuum assumption is valid for microchannels, it can be treated as a normal piping for some cases, either for straight stretches, either for curved sections. So, an approach for entrance conditions in bifurcations of small diameter could be to adopt the classical conditions of developing flow in conventional or thin curved tubes.

As widely discussed (Ghobadi and Muzychka, 2016), it is known that there are still gaps in the area of the flow in curved tubes. The entrance region is one of these cases that is not yet well studied, and no accurate correlation is available to calculate the pressure drop, velocity fields and heat transfer for the developing flow.

Most of the correlations in the not fully developed area are also based on the case studied where the results were limited. Understanding the fluid flow and heat transfer behavior in circular tubes inlet is still an interesting topic for investigations.

Kreulegan and Beiji, 1937, were the first who experimentally studied the flow development in curved pipes. Later, Austin and Seader, 1974, postulated the Eq. (1). They used the angle of tube curvature to obtain fully developed flow for four different coils ($R/a = 6.9, 9.1, 14.4$ and 24.1), where R is the radius of the coil and a is the inner radius of the tube.

$$\varphi = 49 \left(De \frac{a}{R} \right)^{0.33} \quad (1)$$

The Dean Number, De , in the formulation, is given by Eq. (2)

$$De = Re \sqrt{\frac{a}{R}} \quad (2)$$

Equation (1) is valid for $190 \leq De \leq 950$ (Re is the Reynolds Number), and the flow was considered to be hydrodynamically fully developed at the coil entrance and becoming developed because of curvature effects; φ was found around 90 and 245 degrees in most cases, which indicates a very short entrance length.

Newson and Hodgson, 1974, and Yao and Berger, 1975, studied the entrance effects in several conditions, but didn't agree with Eq. (1). On the other hand, Agrawal et al, 1978 and Moulin et al, 2001, found results of good agreement with Austin and Seader, 1974.

Springer et al, 2009, proposed that the length of the developing flow region is determined by the Eq. (3), for low values of Re ($0 \leq Re \leq 400$; $0.25 \times 10^{-3} \text{ m} \leq 2a \leq 2 \times 10^{-3} \text{ m}$ and $4 \times 10^{-3} \text{ m} \leq R \leq 32 \times 10^{-3} \text{ m}$) in toroidal and helicoid thin tubes. Dimensions and variables utilized in their experiences make their work appropriated to a minichannel approach.

$$L = 0.322(2R)^{0.31} Re^{0.59} (2a)^{0.76} \quad (3)$$

Ghobadi and Muzychka, 2009, have done an excellent job on the state of the art of the topic "developing flow in curved ducts". They used several references already cited above and talk about works of Smith, 1974 and 1976, Singh, 1974, Liu, 1977, Humphrey, 1978, Choi et al., 1979, Stewartson et al., 1980, Stewartson and Simpson, 1982, Soh and Berger, 1984, So et al., 1991, and Ebadian et al., 2000, who have developed work in this area of knowledge.

2. MATERIALS AND METHODS

The present work evaluates velocity fields for single phase liquid flows in rectangular bifurcated microchannels entrance. It is considered the flow hydrodynamically fully developed at the entrance and becoming developed because of the effect of the fork. The approach is treating each side of the bifurcation as a curved tube of circular section in a two dimensional analysis, considering only axial and transversal directions.

Classically, it is well known that the velocity field in laminar regime for circular sectioned tubes has a parabolic profile and it is given by the Eq. (4):

$$v_{axial} = \frac{2Q}{\pi r_i^4} (a^2 - r^2) \quad (4)$$

Where Q is the flow rate and a is the inner radius of the pipe (or even the microchannel as assumed herein) and r is the radius as a function of which the velocity varies.

It is assumed in this study that the velocity field will reach the bifurcation and split in two parts, according to the same Eq. (4), however, taking into account the angle θ shown in Fig. 1.

Thus, it might be said that the Eq. (4) will take the shape of the Eq. (5), in the inlet of each side of the bifurcation.

$$v_{axial} = \frac{2Q}{\pi r_i^4} (a^2 - r^2) \cos \pm \theta \quad (5)$$

2.1 Assumption for the Eq. (1) and Eq. (3)

The problem was processed through the Eq. (1) and (3) from Austin and Seader, 1974, and Springer et al, 2009, to find the length of the developing flow region. As these first authors considered the angle φ from the inlet of a torus and, in the present work, the approach is for a bifurcation, Eq. (1) and (3) must be corrected. Considering geometric evidences in the Fig. 1, the Eq. (1) becomes the Eq. (6), because the angle α , from which the not developed flow stretch initiate, shall be the half of the angle φ . Additionally, the inner diameter of the pipe, $2a$, shall be replaced by the hydraulic diameter Dh of the microchannel, according to the classic literature (Bejan, 1993).

$$2\alpha = \varphi = 49 \left(De \frac{Dh}{2R} \right)^{0.33} \quad (6)$$

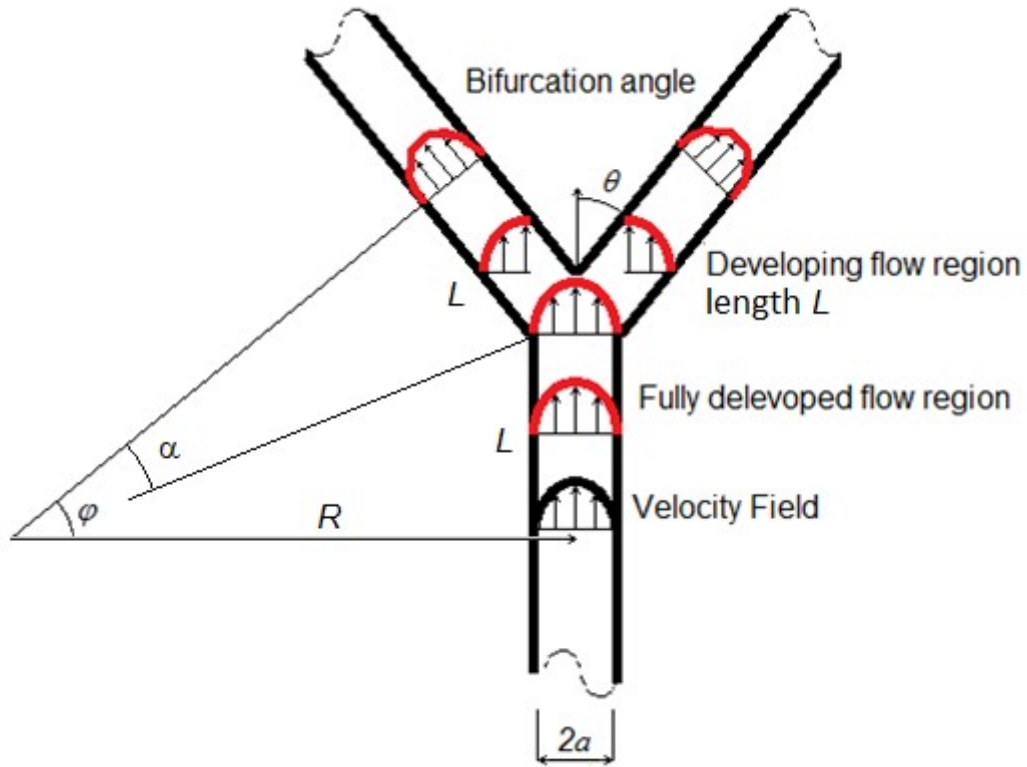


Figure 1. Sketch of a bifurcation in a rectangular sectioned microchannel with an angle θ , showing the developing flow region in the fork entrance.

Once De is given by the Eq. (2) and φ results to be equal θ , The Eq. (6) could be rewritten as:

$$\theta = 49 \sqrt{\frac{Dh}{2R}} (Re)^{0.33} \quad (7)$$

Which gives R as the Eq. (8).

$$R = \frac{1200,5 Dh Re^{0,66}}{\theta^2} \quad (8)$$

For the Eq. (3), other correction must be done. Once the formulation was constructed to translate the length of the developing flow region in a toroidal or helicoid thin pipe and the objective herein is to find the length in a fork of a microdevice, because of geometric constrains evinced in Fig. 1, L must be the half of that original proposed by Springer et al, 2009, and the diameter of the thin pipe must be replaced by the hydraulic diameter Dh of the microchannel. This way, the Eq. (3) becomes Eq. (9).

$$L = 0.161(2R)^{0,31} Re^{0,59} (Dh)^{0,76} \quad (9)$$

2.2 Characteristics and properties of the experimental apparatus

For constant flow rate in the feeder channel, three micro-devices were studied and they are like separation micro-tubes shown in Figs. 2, with water flowing inside under normal conditions of temperature and pressure (NTP). Entrance has 10.30 mm length, 400 μm width and depth of 50 μm , with a larger junction with geometry length of 9.0mm, a width of 400 μm and depth of 50 μm and the thinner channels 9.0mm long, widths of 200 μm , 100 μm and 80 and depth of 50 μm . Input flow rate value was 0.017 ml/min ($2,78 \times 10^{-10} \text{ m}^3/\text{s}$).

The values of main dimensions, flow rate, hydraulic diameter, hydraulic resistance, average speed and Reynolds Number obtained by Avelino et al, 2016, are shown in Tab. 1.

For these micro-devices, the angle of the bifurcation is 60 degrees. Because of geometric reasons, the angle φ , shown in Fig. (1), must be 30 degrees and consequently, α is 15 degrees ($\pi/12$ rad). So, values of R shall be determined by the employment of the Eq. (8) utilizing values given by the Tab 1. The length L , inside what the flow develops, will be determined by the Eq. (9). Calculated values of L were that shown in Tab. 2 and seems to be reasonable, as values of Re are inside the range established as acceptable by Springer et al, 2009, for thin curved tubes.

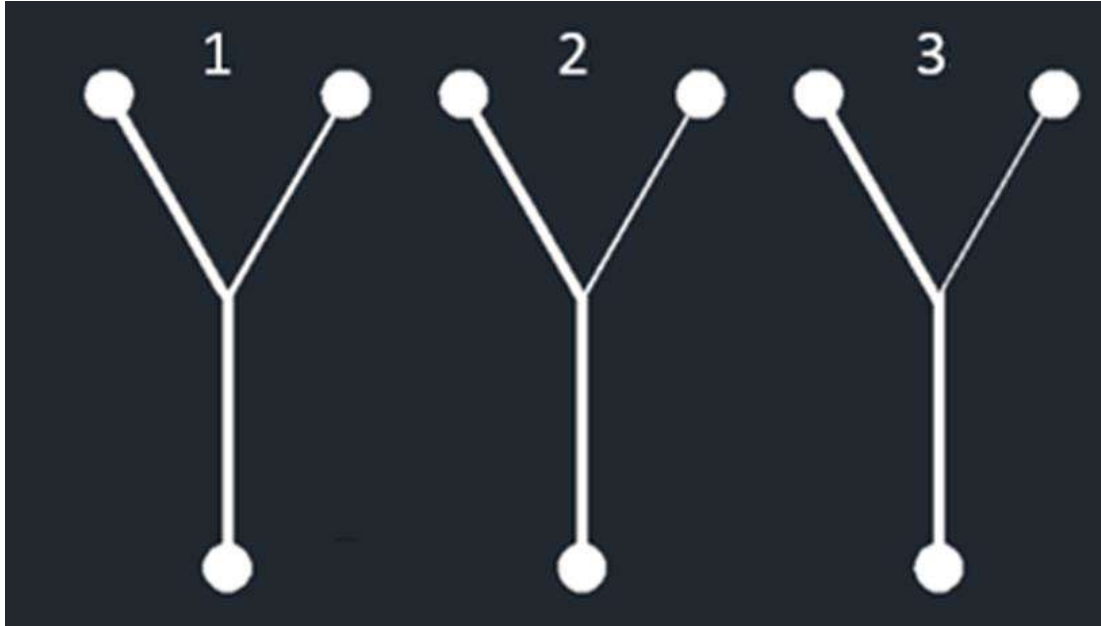


Figure 2. Three micro-devices with different thinner sides.

Table 1. Main dimensions, flow rate, hydraulic diameter, hydraulic resistance, average speed and Reynolds Number about the microchannels proposed and the fluid inside them.

Microchannel	Width (µm)	Length (mm)	Hight (µm)	Flow rate (ml/min)	Dh (µm)	RHydr (Pa.s/m ³)	Av. Sp. (m/s)	Re
In	400	10.30	50	0.0167	88.89	2.48 x 10 ⁻¹²	0.0139	1.23
Out larger 1, 2 & 3	400	9.0	50	0.0145	88.89	5.65 x 10 ⁻¹³	0.0121	1.06
Out thinner 1	200	9.0	50	0.0205	80.00	2.40 x 10 ⁻¹³	0.0080	0.49
Out thinner 2	100	9.0	50	0.0198	66.67	1.90 x 10 ⁻¹³	0.0070	0.46
Out thinner 3	80	9.0	50	0.0024	61.54	1.30 x 10 ⁻¹³	0.0040	0.32

Table 2. Values of Dh and Re given by Avelino et al, 2016, and calculated values of curvature radius R and developing flow region length L.

Microchannel	Dh (µm)	Re	R (mm)	L (m)
Out Larger	88.89	1.06	202.658	0.00013014
Out thinner 1	80.00	0.49	217.730	0.00006287
Out thinner 2	66.67	0.46	173.967	0.00004919
Out thinner 3	61.54	0.32	126.073	0.00003382

2.3 Symmetric bifurcations with variation of angle and flow rate

In terms of variation of velocities and angulations, the input flow rate values in the feeder channel were 0.0085 ml/min (1.39x10⁻¹⁰m³/s) to 10 times it, with a bifurcation half-angle of 45 degrees.

For the angles, they ranged from 15 to 75 degrees, for a larger outlet of 400 µm and a thinner outlet of 200 µm and input flow rate of 2.78x10⁻¹⁰ m³/s.

2.4 Equations governing the problem and assumptions

In order to test conditions of developing flow postulated herein and measure their lengths, equations governing the problem, Eq. (10) to (12), were implemented numerically. Classical mass conservation and momentum equations were treated in Cartesian Coordinates and only two dimensions were considered, where x was the axial direction for any side of the bifurcation and z, the transversal one.

Equation for mass conservation:

$$\frac{\partial v_x}{\partial x} + \frac{\partial v_y}{\partial y} = 0 \quad (10)$$

x Momentum:

$$\rho \left(\frac{\partial v_x}{\partial t} + v_x \frac{\partial v_x}{\partial x} + v_z \frac{\partial v_x}{\partial z} \right) = \rho g_x - \frac{\partial P}{\partial x} + \mu \left(\frac{\partial^2 v_x}{\partial x^2} + \frac{\partial^2 v_x}{\partial z^2} \right) \quad (11)$$

z Momentum:

$$\rho \left(\frac{\partial v_z}{\partial t} + v_x \frac{\partial v_z}{\partial x} + v_z \frac{\partial v_z}{\partial z} \right) = \rho g_z - \frac{\partial P}{\partial z} + \mu \left(\frac{\partial^2 v_z}{\partial x^2} + \frac{\partial^2 v_z}{\partial z^2} \right) \quad (12)$$

For the flow rates entering each side, they were proportional to the flow rate of the microchannel that feed the bifurcation, according to the transversal section of each one, as determined by the mass conservation law. The model did not employ the velocities shown in Tab. 1, experimentally measured by Avelino et al, 2016, but they were calculated inside the simulation, from the respective flow rate.

Boundary conditions were established as velocity zero in the microchannel wall and initial velocity determined by Eq. (5). The mathematical singularity of the corner sharpening between the two sides of the bifurcation was not considered. In contrast, the tip was approached as smoothed.

2.5 Properties of the fluid

As stated above, the fluid flowing inside the microchannel is water in NTP conditions. At this environment, important properties of the water that was considered to calculate velocity fields were density $\rho = 1000 \text{ kg/m}^3$ and dynamic viscosity $\mu = 1,005 \times 10^{-3} \text{ kg/ms}$.

2.6 Simulation Strategy

Relative to the strategy, it is important to highlight that the aim of this work is not to propose an special method of simulation, but to employ it as a tool to test Eq. (9), that search to describe the inlet region of each side of the bifurcation in a microchannel, where the flow is not fully developed.

The simulation was made via finite difference method. It was employed an uniform structured mesh by direction, which seemed to be easier for the case. After several iterations, the mesh chosen for both “out larger” and “out thinner” was one of 1200 x 1200 cells (axial and transversal values). Combinations with more cells led to an excessive time of calculation without any difference in results. For the case of less cells, there were undesirable discontinuities in the final image.

The convergence criterion was 10^{-8} , compared to the relative error and the simulated time ranges were 1, 10, 20, 60 and 600 seconds. However, for periods longer than 1 second, results did not change and 1 second appeared to be adequate.

Only one simulation with step of 10^{-6} seconds was carried out and several with 10^{-5} . Considering that results were not different from those obtained with steps of 10^{-6} seconds and that this simulation took a very long time to go, it was discarded.

A commercial package was employed to generate an image and compare the appearance with that in the simulation made via finite difference method. However, it was not used to measure the length of the region of interest, because the initial conditions postulated in this work are not compatible with that used by this code.

3. RESULTS AND DISCUSSION

With respect to the simulation performed in the commercial package, Fig. 3 shows the result for the micro-device 1, evinced in Fig. 2.

In a closer and more accurate observation on images generated by the commercial package, it is possible to note that the shape of the turbulent region generated by the bifurcation is similar to the scheme shown in Fig.4

Figure 5 shows results of velocity field and the length of the not fully developed flow region, for each bifurcation side of the the micro-device 1 (values of the hydraulic diameter calculated by the authors, not those of Avelino et al, 2016). Tab. 3 shows calculated and measured values for each case.

Table 4 shows results of the not fully developed flow region length, for each bifurcation side, for all three micro-devices studied (values of the width in the second column of the Tab. 1) and three others of smaller widths (highlighted with a symbol *), idealized to verify the behavior of the equation for outlets with dimensions a bit smaller than those of the experimental apparatus elaborated by Avelino et al, 2016.

Figure 6 show the graphical comparison between the calculated values and measured results, for the variation of the widths of the bifurcation outlets.

Results of the simulations, varying only the widths, were between 0.96 and 1.42 times the values calculated through Eq. (9) and recommend that this equation be applied more safely to bifurcations of microchannels with outlets smaller than or equal to 200 μm .

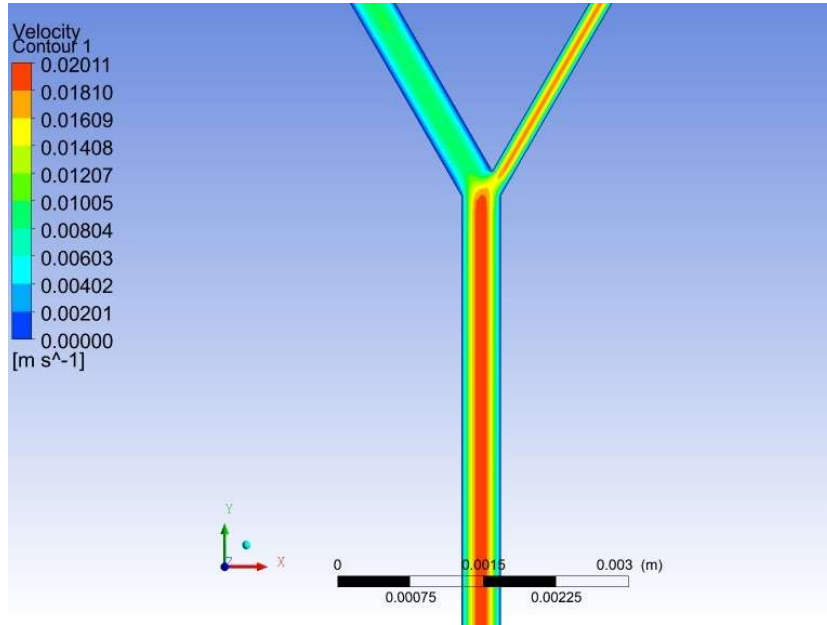


Figure 3. Simulation in commercial package relative to the micro-device 1, showing the appearance of the flow and the distribution of velocities.

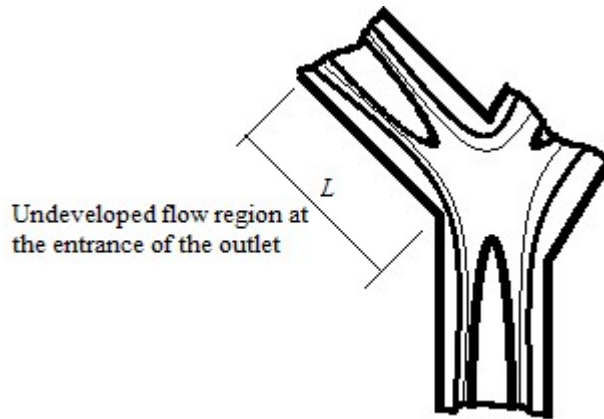


Figure 4. Sketch showing the region of turbulence occurring due to the existence of a bifurcation in a pipe and the length L of the developing flow region at the entrance of one side of the fork.

Table 3. Values of L measured and calculated by Eq. (9).

Microchannel	Dh (m)	Length calculated (m)	Length measured (m)
Out Larger 1	0.00008000	0.00004355	0.00003320
Out Larger 2	0.00008000	0.00005036	0.00003310
Out Larger 3	0.00008000	0.00005202	0.00003180
Out thinner 1	0.00006667	0.00003099	0.00003180
Out thinner 2	0.00005000	0.00002094	0.00003230
Out thinner 3	0.00004444	0.00001736	0.00003260

Results with angle variation can be seen in Tab. 5, they were around 0.59 to 2.31 times those predicted. Notwithstanding, for angles ranging from 30 to 60 degrees, the coincidence was quite reasonable, staying between 0.7 and 1.3 times the predicted. Fig. 7 graphically shows the values of length given by Tab 5.

For an overall flow rate variation between $1,39 \times 10^{-10} \text{ m}^3/\text{s}$ and $1.39 \times 10^{-9} \text{ m}^3/\text{s}$, results can be seen in Tab. 6. Fig. 8 shows the region within which the lengths calculated by Eq. (9) are coincident with the measured values. The equation is, therefore, valid only for flow rates between $1.39 \times 10^{-10} \text{ m}^3/\text{s}$ and $5.56 \times 10^{-10} \text{ m}^3/\text{s}$. In flow rates larger than this range, the values begin to diverge.

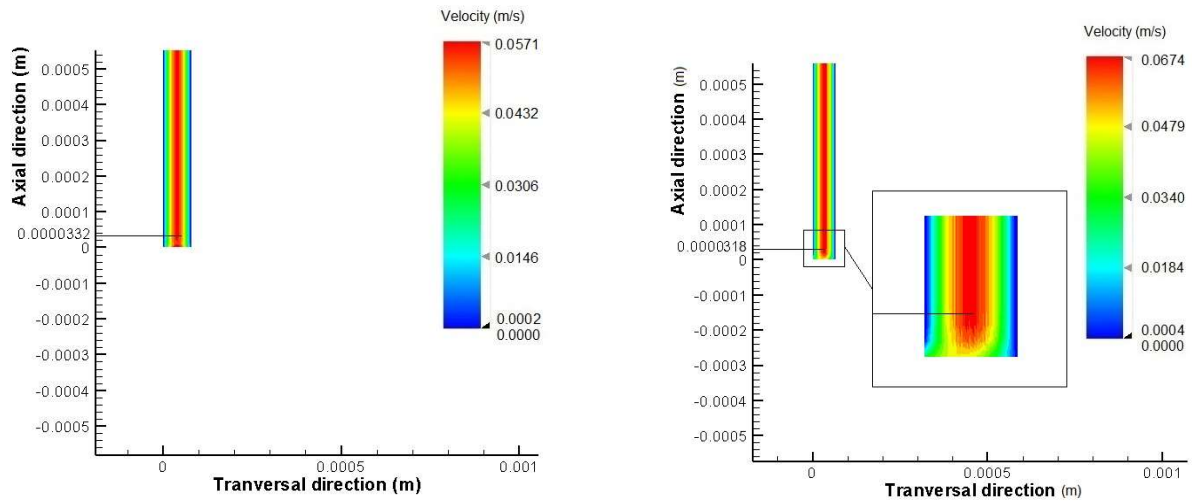


Figure 5. Velocity field in the side “out larger 1*” showing the not fully developed flow region length of 0.0000332 m, in pair with the “out thinner 1*” showing 0.0000318 m (with the detail of the entrance region), both to be compared to the value of L in Tab. 4, third column.

Table 4 Values of L measured and calculated by Eq. (9).

Microchannel	Dh (m)	Length calculated (m)	Length measured (m)
Out thinner 3*	0.00003077	0.00002562	0.00003260
Out thinner 3	0.00004444	0.00001736	0.00002330
Out thinner 2*	0.00003333	0.00002873	0.00003230
Out thinner 2	0.00005000	0.00002094	0.00002950
Out thinner 1*	0.00004000	0.00003668	0.00003180
Out thinner 1	0.00006667	0.00003099	0.00002990
Out larger 1*	0.00004444	0.00004466	0.00003320
Out larger 1	0.00008000	0.00004355	0.00002940
Out larger 2*	0.00004444	0.00004916	0.00003310
Out larger 2	0.00008000	0.00005036	0.00003460
Out larger 3*	0.00004444	0.00005090	0.00003180
Out larger 3	0.00008000	0.00005202	0.00003000

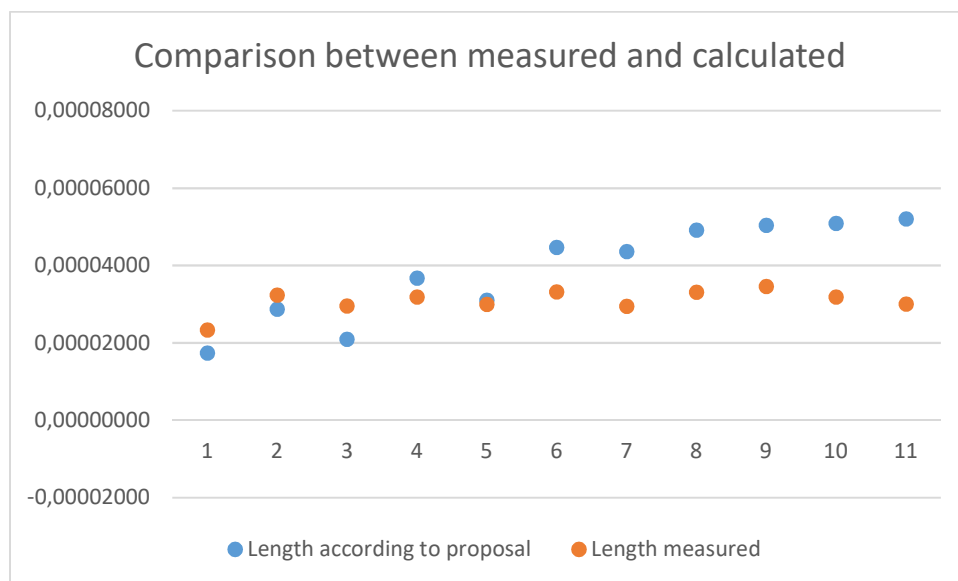


Figure 6. Comparison between measured and calculated values through Eq. (9), for the variation of the widths of the bifurcation outlets.

Table 5. Values of L measured and calculated by Eq. (9), with angular variation.

Microchannel	Flow rate (m ³ /s)	Dh (m)	Angle	Length measured (m)	Length calculated (m)
in	2.78E-10	0.00008000			
out larger	1.85E-10	0.00008000	15	0.0000289	0.0000669
out thinner	9.27E-11	0.00006667	15	0.0000300	0.0000476
out larger	1.85E-10	0.00008000	30	0.0000294	0.0000435
out thinner	9.27E-11	0.00006667	30	0.0000299	0.0000310
out larger	1.85E-10	0.00006154	45	0.0000222	0.0000208
out thinner	9.27E-11	0.00005714	45	0.0000211	0.0000181
out larger	1.85E-10	0.00008000	45	0.0000359	0.0000339
out thinner	9.27E-11	0.00006667	45	0.0000298	0.0000241
out larger	1.85E-10	0.00008000	60	0.0000331	0.0000283
out thinner	9.27E-11	0.00006667	60	0.0000278	0.0000202
out larger	1.85E-10	0.00008000	70	0.0000391	0.0000258
out larger	1.85E-10	0.00008000	75	0.0000367	0.0000247
out thinner	9.27E-11	0.00006667	75	0.0000300	0.0000176

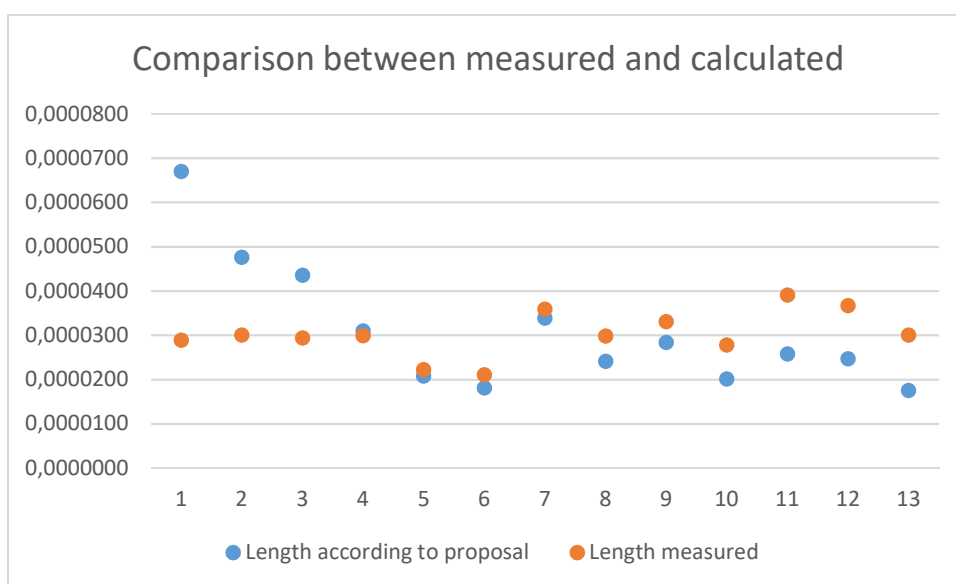


Figure 7. Comparison between measured and calculated values, with variation in bifurcation angle.

Table 6. Values of L measured and calculated by Eq. (9) with flow variation

Microchannel	Flow rate (m ³ /s)	Dh (m)	Angle	Length measured (m)	Length calculated (m)
in	2.78E-10 to 1.39E-9	0.00008000			
out larger	9.27E-11	0.00008000	45	0.00003750	0.00001950
out thinner	4.63E-11	0.00006667	45	0.00001550	0.00001387
out larger	1.85E-10	0.00008000	45	0.00002980	0.00003387
out thinner	9.27E-11	0.00006667	45	0.00003000	0.00002410
out larger	3.71E-10	0.00008000	75	0.00003690	0.00004286
out thinner	1.85E-10	0.00006667	75	0.00003255	0.00003050
out larger	3.71E-10	0.00008000	45	0.00004220	0.00005883
out thinner	1.85E-10	0.00006667	45	0.00002950	0.00004186
out larger	5.56E-10	0.00008000	45	0.00003700	0.00008126
out thinner	2.78E-10	0.00006667	45	0.00003550	0.00005782
out larger	7.41E-10	0.00008000	45	0.00004300	0.00010219
out thinner	3.71E-10	0.00006667	45	0.00002930	0.00007271
out larger	9.27E-10	0.00008000	45	0.00003696	0.00012208
out thinner	4.63E-10	0.00006667	45	0.00003150	0.00008686

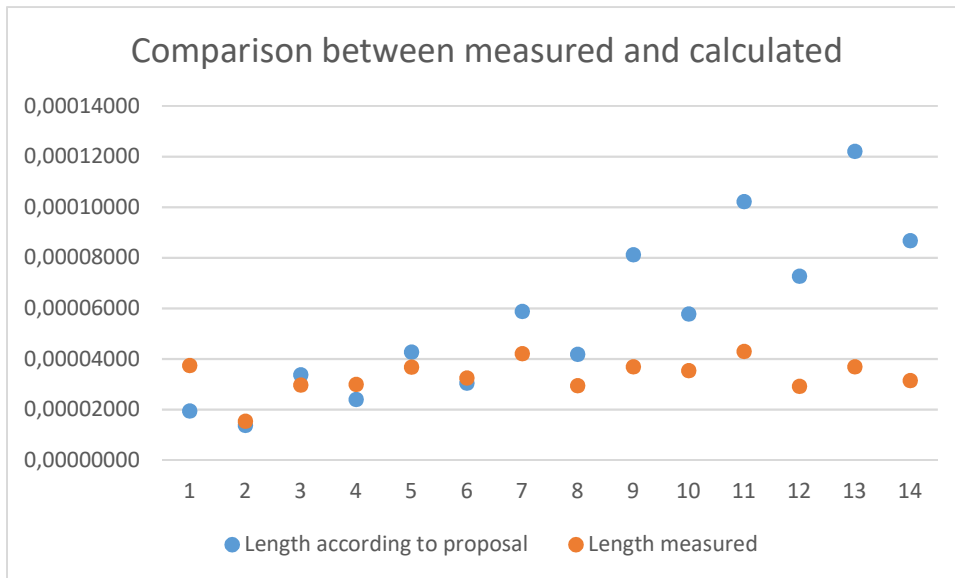


Figure 8. Comparison between measured and calculated values, when there is variation of flow rate in the feeder channel.

Indeed, the applicability of equations developed to describe velocity fields in curved tubes, toward bifurcations was pondered by Pozrikidis, 2012. In preliminary simulations, he showed that the shape of a two-dimensional drop moving through a channel with a fork with sides of parallel walls is similar to that of an axisymmetric drop moving along the center line of a circular tube. So, it is expected that the proposed Eq. (9), as an adaptation of equations for conventional curved tubes and minichannels, could have a good agreement to microchannels.

Calculated values evinced herein showed that, the thinner the side of the bifurcation, the smaller the length of the developing flow region and the smaller the flows and the angles, the smaller the lengths.

It is interesting to note that, according to results of the present work, the undeveloped flow region has a rather small length. This fact was also corroborated by Gongnan et al, 2014. They studied microchannels with symmetric zero-angle bifurcations. The authors did not observe any formation of vortices, but only a small disturbance and a rapid return to laminar condition with increasing speed. Fig.9 shows the phenomenon.

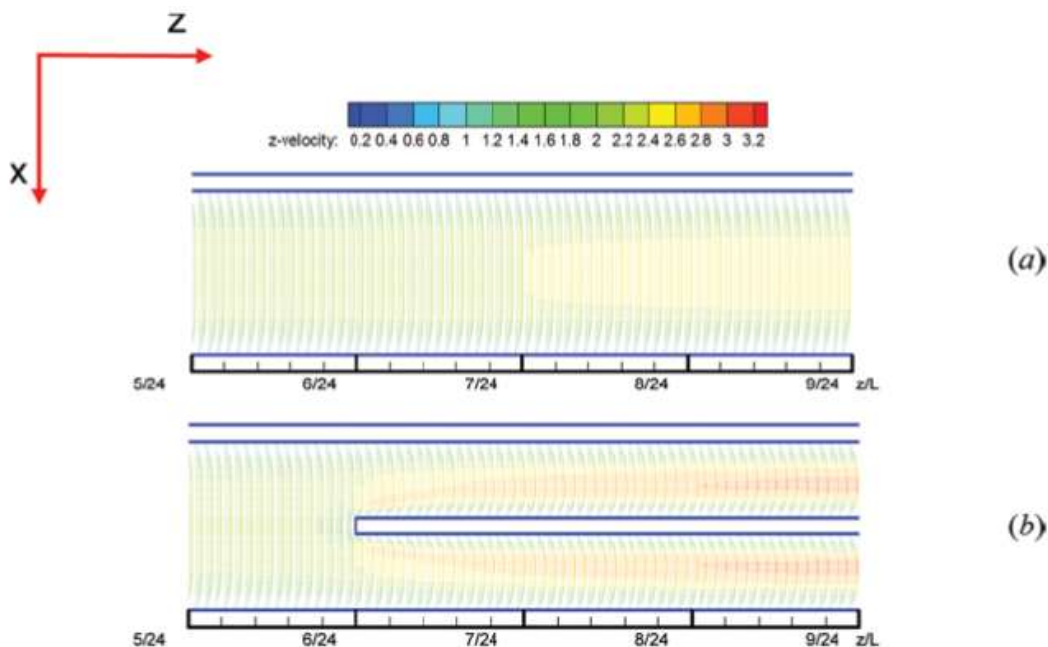


Figure 9. Symmetric zero-angled bifurcation, in a study developed by Gongnan et al, 2014, showing the almost imperceptible effect of the obstacle on the laminar condition of the flow.

4. CONCLUSIONS

Velocity fields of bifurcations in microchannels were verified. Equations developed to predict the length of the developing flow region in curved tubes and minichannels, with water flowing inside at NTP conditions, were tested in microdivisions with different widths, flow rates and angles. An equation was adapted to describe the phenomena in three experimental microdevices.

When varying only the widths, the applicability of this seems to have been better suited to the thinner sides of the bifurcations. The measured length values were between 0.96 and 1.42 times the calculated values. The results obtained in this work recommend that this equation be applied more safely to bifurcations of microchannels with outlets of 200 μm or smaller. In terms of angulation and velocities, the applicability of the equation seems to fit better to the range of bifurcation angles between 30 and 60 degrees and flow rates between $1.39 \times 10^{-10} \text{ m}^3/\text{s}$ and $5.56 \times 10^{-10} \text{ m}^3/\text{s}$.

The extents of the not fully developed flow region found in this work are so small that the flow can be considered fully developed along the entire length of each outlet. This fact is corroborated by Gongnan et al, 2014, who showed that in symmetrical zero-angle bifurcations of rectangular sectioned microchannels, the effect of the obstacle on the laminar flow condition was negligible.

The approach proved to be a good initial path. A more refined analysis can lead to a wider predictability of the proposal, both in dimensional terms (channel widths and bifurcation angles) and for flow rate variation. The applicability of the equation for asymmetric bifurcations must also be tested.

5. ACKNOWLEDGMENT

The authors acknowledge “Programa Pesquisa Produtividade - Universidade Estácio de Sá” for funding the research.

6. BIBLIOGRAPHIC REFERENCES

- Agrawal, Y., Talbot, L., Geong, K., 1978, “Laser Anemometer Study of Flow Development on Curved Circular Pipes”, *Journal of Fluid Mechanics*, vol 85, no 3, pp 497–518;
- Austin, L. R., Seader, J. D., 1974, “Entry Region for Steady Viscous Flowing Coiled Circular Pipes”, *American Institute of Chemical Engineers*, vol 20, pp 820–822;
- Avelino, M. R., Colman, J., Amado, F. P., 2016, “Pressure drop calculation for single phase liquid flows in rectangular bifurcated microchannels”, *Proceedings of the CONEM 2016*;
- Bejan, A., 1993, “Heat Transfer”, Singapore, John Wiley & Sons, Inc., p. 292;
- Cameron, J., Skofronick, J.G., 1978, “Medical physics”, New York, John Wiley & Sons;
- Choi, U. S., Talbot, L., Cornet, E., 1979, “Experimental Study of Wall Shear Rates in the Entry Region of a Curved Tube”, *Journal of Fluid Mechanics*, vol 93, pp 465–489;
- Ebadian, M. A., Zheng, B., Lin, C. X., 2000, “Combined Laminar Forced Convection and Thermal Radiation in a Helical Pipe”, *International Journal of Heat and Mass Transfer*, vol 43, pp 1067–1078;
- Ghobadi, M., Muzychka, Y. S., 2016, “A Review of Heat Transfer and Pressure Drop Correlations for Laminar Flow in Curved Circular Ducts”, *Heat Transfer Engineering*, 37:10, pp 815-839, DOI: 10.1080/01457632.2015.1089735;
- Gongnan, X., Shian, L., Bengt S., Weihong, Z., and Haibin, L., 2014, “A numerical study of the thermal performance of microchannel heat sinks with multiple length bifurcation in laminar liquid flow”, *Numerical Heat Transfer, Part A*, 65: 107–126, DOI: 10.1080/10407782.2013.826084.
- Humphrey, A. C., 1978, “Numerical Calculations of Developing Laminar Flow in Pipes of Arbitrary Curvature Radius”, *American Journal of Chemical Engineering*, vol 56, no 2, pp 151–164;
- Keulegan, G. H., Beiji K H., 1937, “Pressure Losses for Fluid Flows in Curved Pipes”, *Journal of Research of NIST*, vol 18, pp 89–144;
- Liu, N. S., 1977, “Developing Flow in a Curved Pipe”, *INSERM Euromech*, vol 92, pp 53–64;
- Moulin, P., Veyretb, D., Charbit, F., 2001, “Dean Vortices: Comparison of Numerical Simulation of Shear Stress and Improvement of Mass Transfer in Membrane Processes at Low Permeation Fluxes”, *Journal of Membrane Science*, vol 183, no 2, pp 149–162;
- Newson, I. H., Hodgson, T. D., 1974, “The Development of Enhanced Heat Transfer Condenser Tubing”, *Atomic Energy Research Establishment*, vol 14, no 3, pp 291–323;
- Pozrikidis, C., 2012. “Passage of a liquid drop through a bifurcation”, *Engineering Analysis with Boundary Elements* 3, pp 693–103;
- Singh, M. P., 1974, “Entry Flow in Curved Pipes”, *Journal of Fluid Mechanics*, vol 65, no 3, pp 517–539;
- Smith, F. T., 1974, “Pulsatile Flow in Curved Pipes”, *Journal of Fluid Mechanics*, vol 20, pp 820–822;
- Smith, F. T., 1976, “Fluid Flow into a Curved Pipe”, *Proceedings of Royal Society of London, Serial A: Mathematical and Physical Science*, vol 331, pp 71–87;

- So, R. M., Zhang, H. S., Lai, Y. G., 1991, "Secondary Cells and Separation in Developing Laminar Curved-Pipe Flows", *Theoretical and Computational Fluid Dynamics*, vol 3, no 3, pp 141–162;
- Soh, W. Y., Berger, S. A., 1984, "Laminar Entrance Flow in a Curved Pipe", *Journal of Fluid Mechanics*, vol 148, pp 109–135;
- Springer, F., Carretier, E., Veyret, D., Moulin, P., 2009, "Developing Lengths in Woven and Helical Tubes with Dean Vortices Flows", *Engineering Applications of Computational Fluid Mechanics*, 3:1, 123-134, DOI:10.1080/19942060.2009.11015259
- Stewartson, K., Cebeci, T., Chang, K. C., 1980, "A Boundary Layer Collision in a Curved Duct", *The Quarterly Journal of Mechanics and Applied Mathematics*, vol 33, pp 59–75;
- Stewartson, K., Simpson, C. J., 1982, "On a Singularity Initiating a Boundary-Layer Collision", *The Quarterly Journal of Mechanics and Applied Mathematics*, vol 35, pp 1–16;
- Yao, L. S., Berger, S. A., 1975, Entry Flow in a Curved Pipe, *Journal of Fluid Mechanics*, vol 67, no 1, pp 177–196;

7. RESPONSIBILITY NOTICE

The authors are the only responsible for the printed material included in this paper.